Acoustic Waveform Singularities from Supersonic Rotating Surface Sources

Valana L. Wells*
Arizona State University, Temple, Arizona 85287

This paper discusses the analytical characteristics of waveforms produced by rotating surface sources with tip Mach number >1. The analysis covers both monopole and quadrupole sources that have the greatest importance for prediction of high-speed rotor noise. By using idealized source distributions over the rectangular surfaces, it is shown that the Lighthill/Curle analogy with time derivatives taken outside the integrals poses no additional difficulty attributable to numerical error. The integrals themselves require careful analysis of critical points in the integrand so that an adaptive integration grid can be developed for each time step. A mathematical analysis of the integrands arising from the idealized sources predicts a logarithmic singularity at critical points in the monopole waveform and a single-pole singularity at such points in the quadrupole waveform. The computation bears out these predictions.

Introduction

THE method outlined by Ffowcs Williams and Hawkings[1] for calculating the acoustic pressure resulting from aerodynamic sources has become the standard in the study of rotor noise prediction. Though an extremely useful formulation for many applications because it is derived for a frame of reference moving with the noise source, the most well-known form of the equation is not easily used to predict rotor noise any time the rotor tip Mach number becomes ≥ 1. This results from the singularities in the source integrals that occur at $M_r = 1$, where M_r is the component of the source Mach number in the direction of the observer. Fortunately, the singularity is integrable, and the equation can be rewritten in terms of integrals over what, in Farassat's[2] parlance, is termed the Σ surface, but here will be called just the "acoustic planform."

Farassat[3,4] has previously developed a reformulation of the Ffowcs Williams-Hawkings equation in which the derivatives that operate on the linear source integrals are taken under the integral sign. His more recent work develops the same type of formulation for the quadrupole sources.[5,6] Farassat has taken this approach because, as he points out, the functions in question are sensitive to observer time, particularly near $M_r = 1$; therefore, numerical time differentiation of them is prone to error. In general, moving the derivatives inside the integral will strengthen singularities in the integrand, and only clever mathematical manipulation on the part of Farassat has produced forms usable in numerical calculations. However, even with these advances, it appears that the calculation remains sensitive. The pressure-time plots shown, for example, in Ref. 4 illustrate that, though greatly improved, the general waveforms still exhibit the lack of smoothness expected in an analytical presentation.

Amiet[7] discusses the relative merits of treating the integrals in the acoustic analogy formulation with the derivative outside the integral sign vs taking the derivative under the integral. Amiet contends that it is preferable to take the derivative first in order to alleviate the supposed difficulties involved with numerically differentiating a numerically computed integral. As will be shown, the difficulties are actually in the integration itself, and, except in regions of true singularities, there is no problem with numerically differentiating the curve resulting from the computed integrations.

With the preceding points as motivation, then, the current paper studies the sensitivity of the source integrals for rotating surfaces, such as rotor blades, with tip Mach numbers >1. The development describes a method for computing those integrals, which here have been retained in their "acoustic analogy" forms. As expected, the integrals show great sensitivity to time in the region near $M_r = 1$ for all supersonic spanwise locations along the surface. To handle this sensitivity, each radial station at which $M_r = 1$ must be determined for all time steps in the calculation. Then an integration grid must be fitted so that it clusters integration points near those critical radii. The characteristics of the problem necessitate computing a new grid for every time step, but using this technique virtually eliminates the "noise" in the computed waveform, even after taking the numerical derivative. To keep the analysis as simple as possible, the following development and results are strictly valid only for thin surfaces in the far field.

Development

The simplest form of the acoustic analogy describing the thickness noise produced by a foreign body in motion is given by

$$p'(x, t) = \frac{1}{4\pi}\frac{\partial}{\partial t}\int_S \frac{\rho_0 v_n(y, \tau)}{|x - y|}\,dS(y) \tag{1}$$

where x and y are the observer and source locations, respectively; v_n the normal velocity to the surface; and p' the disturbance pressure. It is convenient to make this equation dimensionless. If distances are nondimensionalized by the factor Ω/a, where Ω is the constant angular velocity of the rectangular surface and a the speed of sound, then the dimensionless radius of a point on the surface is simply its rotational Mach number. For this reason M will be used to designate the dimensionless radial coordinate; it also implicitly gives the rotational Mach number of that radial station. Converted to a cylindrical coordinate system, which better handles the geometry associated with a rotating surface source, the equation becomes

$$2\pi C_p = \frac{\partial}{\partial \tilde{t}}\int\int\left[\frac{M_n}{\tilde{r}}\right]M\,d\psi\,dM \tag{2}$$

Received May 9, 1989; revision received Feb. 12, 1990.

*Assistant Professor, Department of Mechanical and Aerospace Engineering. Member AIAA.

where $\tilde{t} = \Omega t$, $C_p = p'/\frac{1}{2}\rho_0 a^2$, M the rotational Mach number of a radial position on the source (dimensionless radius), and $\tilde{r}$ the dimensionless distance between a point on the acoustic planform and the observer. M_n is now the Mach number normal to the surface, and ψ the angular position of a point on the acoustic planform. The distance $\tilde{r}$ is determined geometrically. With reference to Fig. 1,

$$\tilde{r} = \sqrt{M^2 + R^2 + 2MR\cos\psi} \tag{3}$$

Note that all distances are made dimensionless by the factor Ω/a. The emission time τ is just ψ/Ω, and R represents the dimensionless distance between the observer and the center of rotation (hub).

The brackets in Eq. (2) indicate that the integrand must be evaluated at the emission time τ. In addition, the quantity $M\,dM\,d\psi$ represents a dimensionless differential surface element in cylindrical coordinates that must be taken over the acoustic planform. The planform is generated through the expression $g = 0$, where

$$g = \psi - \tilde{t} + \tilde{r} \tag{4}$$

This is simply the particular expression for (the negative of) the retarding function, often written as

$$g = t - \tau - \frac{|x - y|}{a}$$

To complete the description of the surface, the equation $g = -\delta$ must be solved, where δ represents an angular offset; if, for example, the leading edge of the surface is at $\psi = 0$ when $\tau = 0$, the trailing edge would be located at $\psi = -\delta(M)$ at the same τ (see Fig. 1).

Since evaluation of the integrand must take place at (y, τ), it is necessary to express M_n in such terms. Assuming that the surface of the rotating body is rigid so that its location in its own frame does not depend on time, a function describing the location of a rotating surface has the general form in cylindrical coordinates:

$$f = f(r, \psi - \Omega t) \tag{5}$$

Evaluated at $\tau = t - |x - y|/a$, this gives $f = f(r, \psi - \tilde{t} + \tilde{r})$, or $f = f(r, g)$. Therefore, the expression for M_n in dimensionless coordinates can be considered a function of M and g under the integral sign.

Since the usual acoustics problem does not consider the case of coincident source and observer, $\tilde{r} \neq 0$, and the integrand of the acoustic analogy equation given earlier is never singular. It appears straightforward, then, to employ some quadrature method to numerically evaluate the known integrand over the computed acoustic planform. However, it is well-recognized that such an integration followed by numerical differentiation results in an acoustic signature prediction that is not smooth and is difficult to interpret. An example of this, shown in Fig. 2a, is taken from Ref. 8. Figure 2b, on the other hand, illustrates the noise signature from the same rotor under the same operating conditions but using the newly derived method for computing the integrals. The derivative is numerically computed using a simple two-point differencing scheme. The waveform exhibits the smooth, well-behaved character expected for this analytical solution.

To obtain the smooth result pictured in Fig. 2b, a careful study of the behavior of the function g is required. As pointed out previously, the solution of $g = 0$ gives the location of all points on the acoustic planform. Solving $g = 0$ for $\psi(\tilde{t})$ gives solutions resembling those shown in Fig. 3 for three different observer times. The rotating surface used to generate the illustrated planforms has an aspect ratio of 14 and a tip Mach number equal to 1.5. The observer for this case is located at three radii ($3M_{tip}$) from the center of rotation and is in the plane of rotation. Notice that with this supersonic tip Mach number the acoustic planform becomes non-simply-connected at certain observer times. This phenomenon arises when some location on the surface leading or trailing edge passes through the position where its Mach number is in the direction of the observer (M_r) equals 1. Multiple acoustic planform regions occur only when $M_r > 1$ for leading- or trailing-edge points. Furthermore, when both the leading *and* trailing edges have $M_r > 1$ (at some outboard radial position), the planform becomes connected once again, but with the characteristic "dips" near the tip, as illustrated in Fig. 3c.

It is illustrative to study the function $g = 0$ as a function of observer time $\tilde{t}$ for some radial location M. Consider a test case in which the rotating surface, or blade, has an aspect ratio of 14 and a tip Mach number of 1.5. The observer is in the rotor plane at a dimensionless distance $R = 4.5$ from the rotor hub. Figure 4 shows the relationship between observer time and emission angle for several radial locations on the surface. Each plot contains a solid line representing the solution to $g = 0$ for the surface leading edge and a dashed line for the surface trailing edge [$g = \delta(M)$]. A horizontal line at a given value of $\tilde{t}$ between the solid and dashed curves delineates the extent of the acoustic planform chord at the radial location in question. Note the distinct difference between the shapes of these curves in the subsonic and the supersonic ranges. As long as the rotational Mach number remains < 1, each g equation has only one root. However, for supersonic speeds, three roots are present for a range of observer times, and, most significantly, there are two distinct solutions to the equation at two observer times for each supersonic curve. These times with two separate emission angles represent the times corresponding to the transition from $M_r < 1$ to $M_r > 1$. Consequently, $M_r = 1$ at the times in question.

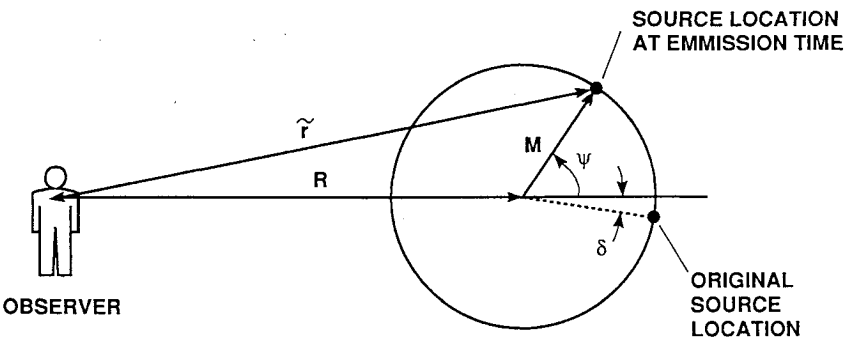

Fig. 1 Geometry for acoustic planform computation: dimensionless variables.

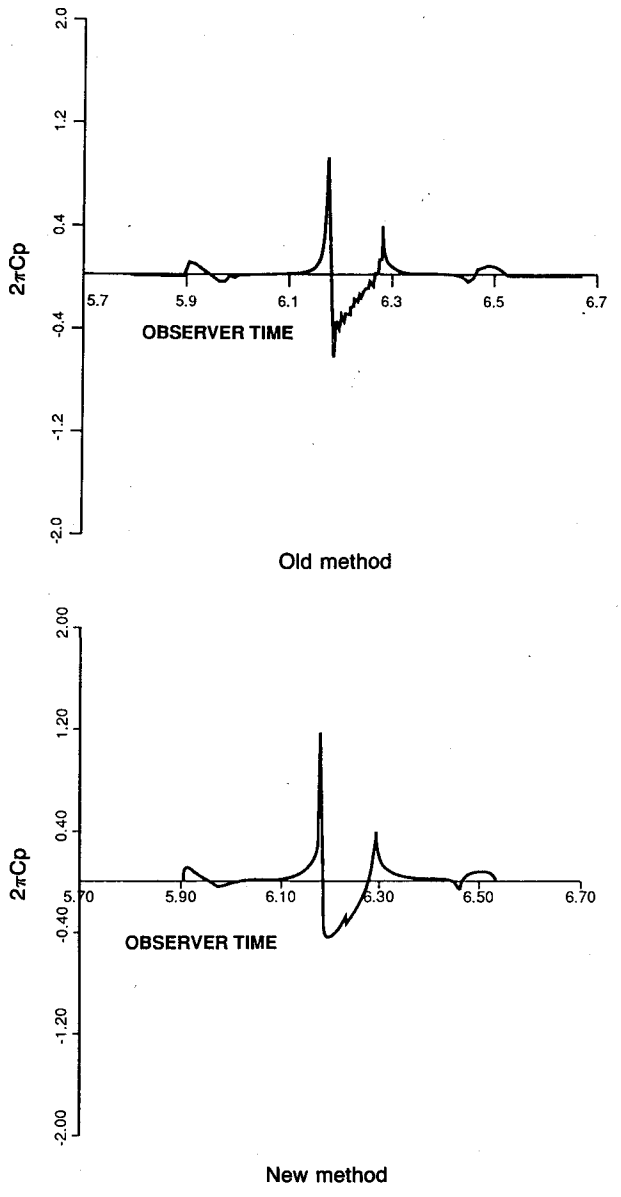

Fig. 2 Acoustic waveforms: comparison of old and new methods.

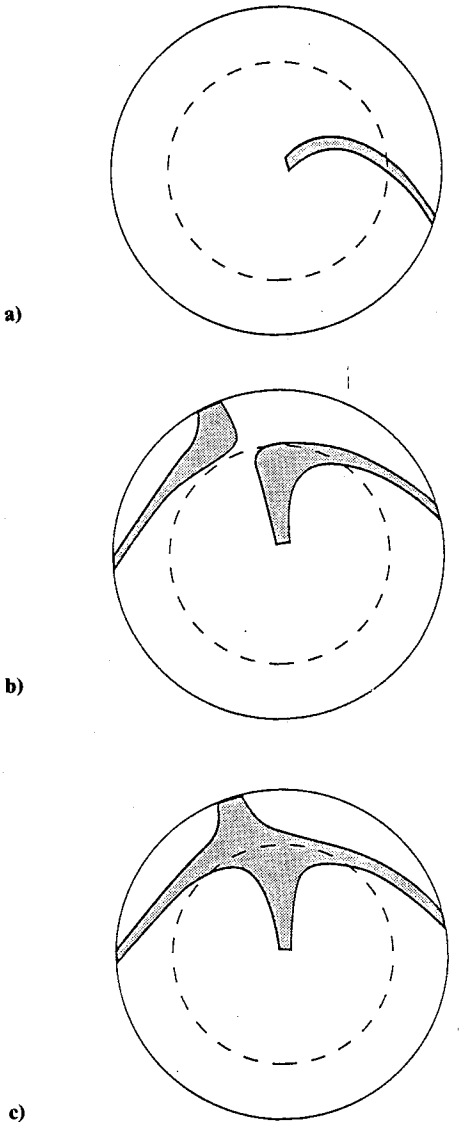

Fig. 3 Typical acoustic planform shapes: supersonic tips.

To appreciate the significance of the preceding observations, an expression for M_r is obtained geometrically. Recalling that M_r is the component of the source Mach number, M, in the direction of the observer, a simple geometric construction gives

$$M_r = \frac{MR \sin\psi}{\tilde{r}} \tag{6}$$

Now, finding the extrema of g with respect to ψ results in

$$\frac{\partial g}{\partial \psi} = 0 = 1 + \frac{\partial \tilde{r}}{\partial \psi} = 1 - \frac{MR \sin\psi}{\tilde{r}} \tag{7}$$

Comparing Eq. (7) with Eq. (6) leads to the condition that $M_r = 1$ at the local maximum and minimum points on those curves representing $g = 0$ for supersonic rotational speeds. At all times between these extrema, $M_r > 1$ at one of the three emission angles (the middle one), and $M_r < 1$ at the other two. The three roots come about because the source effectively outruns and then is passed by its own acoustic wave. This process is essentially the same for all supersonically traveling sources. A variation in the order of leading- and trailing-edge critical points (i.e., times at which $M_r = 1$) occurs depending on the Mach number of the radial station, the distance to the observer, and the surface chord length. In comparing Figs. 4c and 4d, for example, it can be seen that, for the lower Mach number station, the leading edge enters and leaves the supersonic region before the trailing edge relative Mach number becomes >1. Figure 4d, however, shows a case where both leading and trailing edges are supersonic at the same time.

Regardless of the observer time, as long as some portion of the rotating surface has a Mach number in the observer direction ≥ 1, there will be a transition from one to two to three roots of $g = 0$ at some radial position. From the plots in Fig. 4 it is apparent that a large change in acoustic planform chord, and therefore in area, will occur at these loci. Thus, an integration covering the planform, necessarily including the transition radii, must carefully consider these points of rapid change of chord. To implement an accurate numerical integration scheme, grid points must be clustered in these regions, in much the same way that grid points for finite differencing are clustered in areas of large gradients in the flowfield. These "critical points," in both the mathematical and colloquial sense, always occur when $M_r = 1$ at the leading or trailing

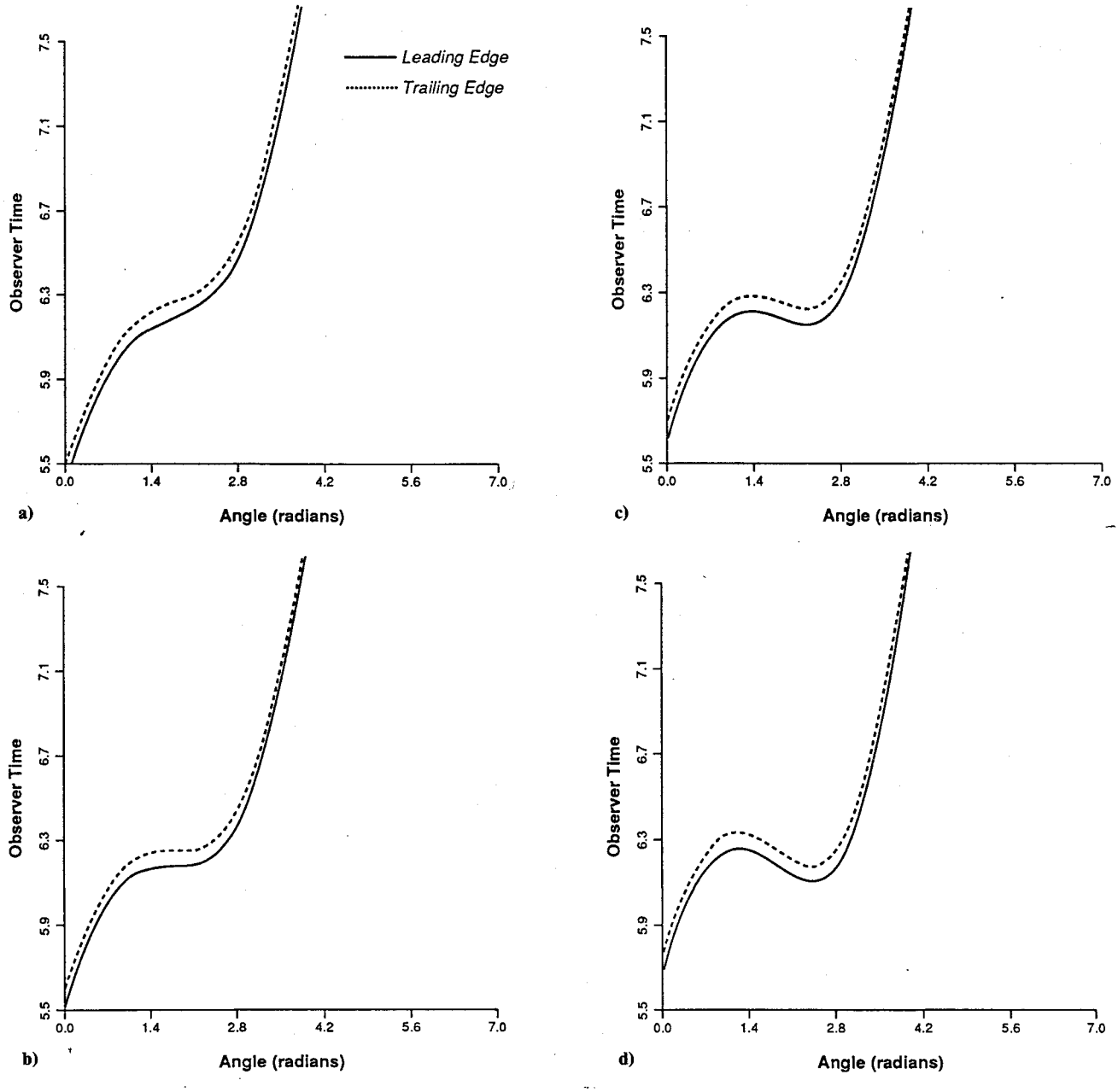

Fig. 4 Observer time vs acoustic planform position: varying radial locations: a) $M = 0.9$; b) $M = 1.0$; c) $M = 1.1$; d) $M = 1.2$.

edge of the surface. Furthermore, at any observer time when any part of the surface is supersonic, there will be at least one unique critical point. Therefore, a new grid must be generated for every time step during the supersonic portion of the surface's sweep. Figure 5 shows the results for a thickness noise pressure pulse for a rectangular surface rotating with tip Mach number of 1.1 with an aspect ratio of 12 and a 10% parabolic arc chordwise thickness distribution. The observer is located in plane at 10 diam from the center of rotation. This is the precise case tested by Amiet,[7] and the waveform correlates exactly with his calculation. As pointed out previously, the current prediction uses simple numerical differentiation and requires no integration over singularities. The only infinities arise when $M = 1$ and $M_r = 1$ for both leading and trailing edges; this is characteristic of Amiet's results as well and is discussed in the section on true singularities in the waveform.

Monopole Results

Figure 6 shows results from integrating Eq. (2) for a rectangular surface with an aspect ratio of 14 and a NACA 0012 airfoil section. The section is modified to avoid the infinite slope of the leading edge. All waveforms exhibit features that Amiet calls "near-singularities." These appear as discontinuities in the waveform and occur when the rotor tip leading and trailing edges enter and leave the supersonic region. The effect is not unexpected since, as shown by studying Figs. 3 and 4, a significant change occurs in the shape and area of the acoustic planform at these times. These points of near-singularity are predominant in the waveform for tip Mach numbers of 1.05 and 1.1. For these two cases there are particularly large changes in the acoustic planform shape at the times of interest.

In examining Fig. 6 it becomes evident that, at some critical tip Mach number, the amplitude of the pressure disturbance begins to decrease. In other words, there is a tip Mach number that produces a maximum pressure disturbance. This M_{tip} is a function of surface aspect ratio and observer location and corresponds to the Mach number at which the trailing edge becomes supersonic (relative to the observer) at the same time that the leading edge leaves the supersonic region. Note that this phenomenon does not arise directly because of the

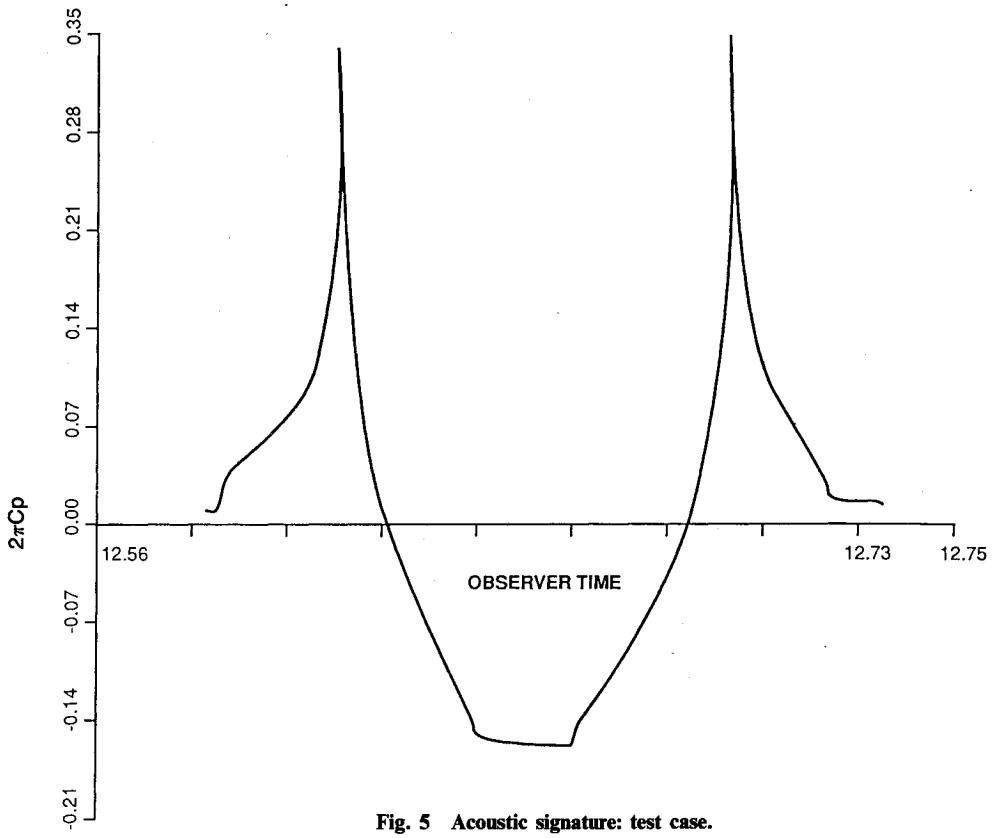

Fig. 5 Acoustic signature: test case.

Doppler factor, $1/|1-M_r|$, which appears in some formulations of Eq. (2). This is evident since, as long as the tip travels faster than the speed of sound, there will be some location on the surface with $M_r = 1$.

Quadrupole Results

In the preceding case the source strength is distributed smoothly over the surface in the chordwise direction so that no sudden changes in the monopole strength occur from the leading to the trailing edge. The monopole distribution is particularly simple, and, when considering the more complex quadrupole source distributions resulting from, for example, shock-wave formation on and beyond the tip of the rotating surface, the grid computation becomes more complicated. In particular, the grid must now include the $M_r = 1$ radius for the chordwise shock-wave location as well as those for the leading and trailing edges.

In the acoustic far field the quadrupole noise is determined through solution of the following integral equation:

$$4\pi p'(x,t) = \frac{1}{a^2}\frac{\partial^2}{\partial t^2}\int_V \left[\frac{T_{rr}}{r}\right] \mathrm{d}V(y) \tag{8}$$

The preceding integral is carried out over all space at the retarded time. T_{rr} is the component of the Lighthill stress tensor in the observer direction. A simplified approximation for T_{rr} has been suggested by Schmitz and Yu,[9] who claim that, for quadrupole sources localized near the tip of the rotating surface and with an in-plane observer,

$$T_{rr} \approx \rho_0 u^2\left(1+\frac{\gamma-1}{2}M^2\right) \tag{9}$$

where u is the local chordwise velocity. In dimensionless form, with distances nondimensionalized by Ω/a and $\tilde{t} = \Omega t$,

$$2\pi C_p = 4\frac{\partial^2}{\partial \tilde{t}^2}\int_V \left[\frac{C_p^2\left(1+\frac{\gamma-1}{2}M^2\right)}{M^2\tilde{r}}\right] \mathrm{d}V(y) \tag{10}$$

C_p is again made dimensionless by $1/2\rho a^2$, and the preceding substitution is only valid for thin surfaces.

Observing that the out-of-plane extent of T_{rr} is almost negligible using the previously given approximation, it can be surmised that the retarded time of a source point above the plane of rotation is approximately equal to that of a point on the plane. In other words, $\tilde{r}$ is approximately not a function of $\tilde{z}$. With this assumption in mind it can be argued with the aid of supporting experimental data that the integration in the $\tilde{z}$ direction will not change the basic shape of the chordwise distribution of pressure on the surface. Specifically, the sharp increase in C_p characteristic of a shock wave will remain even after the integral in the axial direction is taken. Accepting the validity of this argument, the approximated quadrupolar pressure coefficient can be written as

$$2\pi C_p = 4\frac{\partial^2}{\partial \tilde{t}^2}\int_S \frac{\tau(g,M)}{\tilde{r}} \mathrm{d}S(y) \tag{11}$$

where now

$$\tau(g,M) = \int_{-\infty}^{\infty} \frac{C_p^2\left(1+\frac{\gamma-1}{2}M^2\right)}{M^2} \mathrm{d}\tilde{z} \tag{12}$$

Because of the generic shape of the C_p distribution, τ will have a discontinuity in slope at $g = 0$ and a discontinuity in the function itself at $g = -\xi$, where ξ corresponds to a shock location (or other discontinuity) on the surface.

An approximation to the shape of a typical C_p distribution on the surface of a rotor blade was used as a source in the calculation that produced Fig. 7. Because the source amplitude and shape are modeled only approximately, the absolute pressure coefficients are meaningless; however, the waveform shape shows some similarities to experimental measurements, and the curve is, again, virtually without the spikiness previously encountered even after two numerical derivatives. However, a disturbing trend is the singular behavior once again

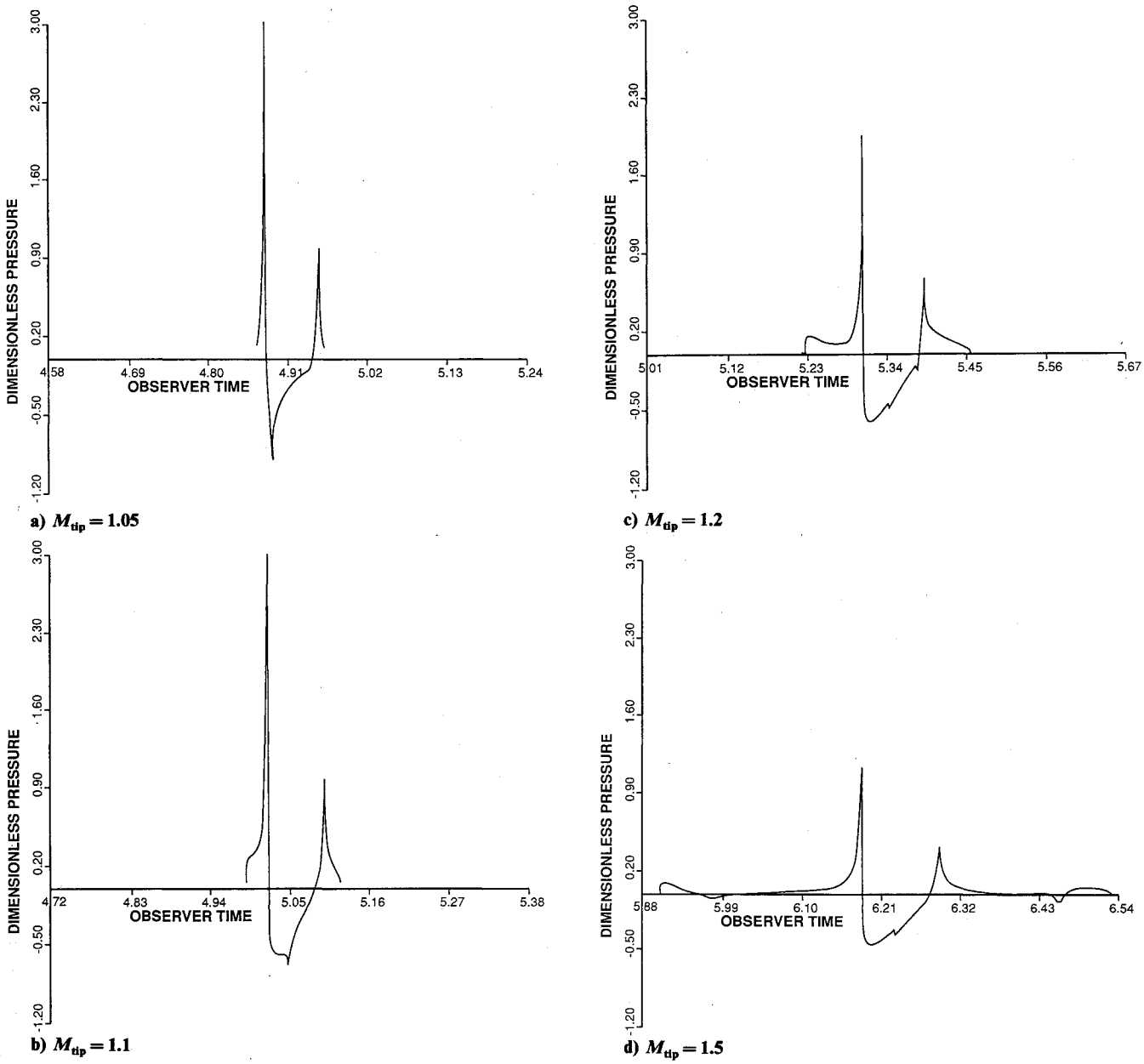

Fig. 6 Monopole waveforms.

encountered. The very strong singularity shown in the figure occurs at an observer time corresponding to the condition that the shock wave that is traveling at a rotational Mach number of 1 also has a velocity relative to the observer of 1. This result is a consequence of the linear propagation assumption and provides evidence that the quadrupole approximation proposed by Schmitz and Yu[9] cannot account for at least some of the important nonlinear effects.

Singularity Analysis

Both monopole and quadrupole waveforms exhibit singular behavior at observer times corresponding to $M = 1$, $M_r = 1$ for leading and/or trailing edges. Amiet[7] discusses the singular behavior for monopole noise. The following development, by taking a more general approach, addresses the singularity in the quadrupole calculation and reaches the same conclusion as that of Amiet with regard to the monopole singularity.

The analysis proceeds by first showing that both monopole and quadrupole integrals can be written in essentially the same form. Note the M_n in the numerator of the monopole

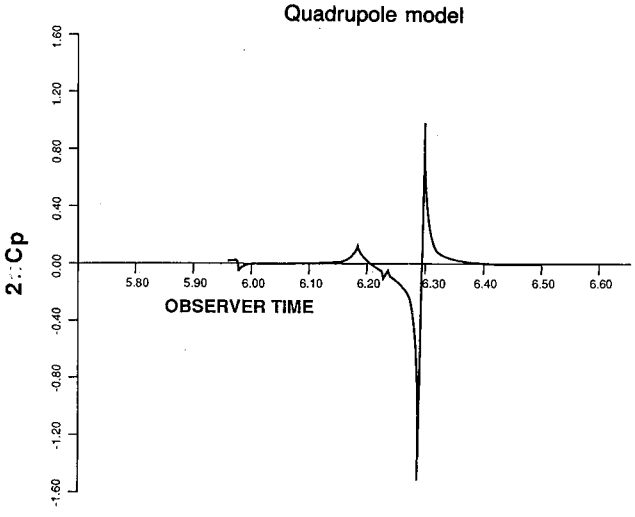

Fig. 7 Acoustic waveform using quadrupole model.

integrand [Eq. (1)] is, for thin surfaces, simply $M\,\partial y/\partial\psi$, where $y(\psi)$ represents an equation for the thickness of the surface at a constant radius. Then, under the integral sign M_n can be written as $h'(g,M)$, where g, the retarding function, has replaced the original ψ. The prime refers to differentiation with respect to g.

From the definition of g found in Eq. (4) the derivative $-\partial/\partial g$ can interchange with $\partial/\partial\tilde{t}$. Taking the derivative under the integral sign then gives

$$2\pi C_p = -\int_S \frac{h''}{r}\,\mathrm{d}S(y) \tag{13}$$

Applying the appropriate equivalent procedure to the quadrupole integral, Eq. (11), results in exactly the same expression as in Eq. (13), but now with

$$h'' = \tau''$$

Thus, h can be thought of as some source distribution across the chord of the surface; its value and shape depend on whether h models a monopole or a quadrupole distribution. For the monopole case h has a discontinuity in slope at $g = 0$ and $-\xi$, but is continuous in the function itself. When h models a pressure distribution with shock wave, the function has a discontinuity at $g = -\xi$ corresponding to the sharp jump in pressure across the shock. It is additionally noted that, since all calculations considered here are in the far field, the r in the integrand denominators will not contribute to the singularities; thus, further development will consider integrals of the form $\int h''\,\mathrm{d}S$.

The function h is nonzero between 0 and $-\xi$ and can be expressed as

$$h(g) = \bar{h}(g)[-H(g) + H(g+\xi)] \tag{14}$$

where H represents the Heaviside step function. The variable ξ could be $\delta(M)$, the location of the trailing edge, or for quadrupole models, the chordwise shock location. Letting $[H] \equiv [-H(g) + H(g+\xi)]$ and $[\delta] \equiv [-\delta(g) + \delta(g+\xi)]$ (now $\delta \equiv$ the Dirac delta function),

$$h'' = \bar{h}''[H] + 2\bar{h}'[\delta] + \bar{h}[\delta'] \tag{15}$$

The prime on δ means differentiation with respect to its argument.

As discussed earlier, $\mathrm{d}S(y) = M\,\mathrm{d}\psi\,\mathrm{d}M$, where the limits on ψ go from $-\infty$ to ∞ and on M from 0 to $M_{\max}$. Taking the ψ integral first gives

$$\int_{-\infty}^{\infty} \bar{h}'[\delta]\,\mathrm{d}\psi = \int_{-\infty}^{\infty} \bar{h}'[\delta]\frac{\mathrm{d}g}{\left|\frac{\partial g}{\partial\psi}\right|} = \left.\frac{\bar{h}'}{\left|\frac{\partial g}{\partial\psi}\right|}\right|_{g=0,-\xi} \tag{16}$$

and, using an identity from Gel'fand and Shilov,[10]

$$\int_{-\infty}^{\infty} \bar{h}[\delta']\,\mathrm{d}\psi = -\left.\frac{1}{\left|\frac{\partial g}{\partial\psi}\right|}\right|_{g=0,-\xi} \int_{-\infty}^{\infty} \frac{\partial}{\partial\psi}\left(\frac{\bar{h}}{\frac{\partial g}{\partial\psi}}\right)[\delta]\,\mathrm{d}\psi$$

$$= -\left.\frac{\bar{h}'}{\left|\frac{\partial g}{\partial\psi}\right|} + \frac{\bar{h}}{\left(\frac{\partial g}{\partial\psi}\right)^2}\frac{\frac{\partial^2 g}{\partial\psi^2}}{\left|\frac{\partial g}{\partial\psi}\right|}\right|_{g=0,-\xi} \tag{17}$$

Now using Eqs. (16) and (17) to integrate $\int h''\,\mathrm{d}S$ gives

$$\int_S h''\,\mathrm{d}S(y) = \int_0^{M_{\max}}\int_0^{-\xi} \bar{h}''\,\mathrm{d}\psi M\,\mathrm{d}M + \int_0^{M_{\max}} \left.\frac{\bar{h}'}{\left|\frac{\partial g}{\partial\psi}\right|}\right|_{g=0,-\xi} M\,\mathrm{d}M + \int_0^{M_{\max}} \left.\frac{\bar{h}\frac{\partial^2 g}{\partial\psi^2}}{\left|\frac{\partial g}{\partial\psi}\right|}\frac{1}{\left(\frac{\partial g}{\partial\psi}\right)^2}\right|_{g=0,-\xi} M\,\mathrm{d}M \tag{18}$$

This can be considered as three integrals, the first of which is always nonsingular. The other two integrals, I_2 and I_3, respectively, will have singularities when $\partial g/\partial\psi = 0$ at $g = 0$ or $-\xi$. Notice that $I_3 = 0$ when only monopole sources are present, since the form of source distribution will require that $h = 0$ when $g = 0$ or $-\xi$.

Expanding the derivative $\partial g/\partial\psi$ in a Taylor series about the singular point (M_0,ψ_0) leads to

$$\frac{\partial g}{\partial\psi} = C_1\Delta\psi + C_2\Delta M + \cdots \tag{19}$$

since $\partial g/\partial\psi = 0$ at (M_0,ψ_0). Equation (19) is written after the fashion of Amiet. To find the relationship between ΔM and $\Delta\psi$, expand the function g about the singularity, keeping in mind that $g = \text{const}$:

$$g(M,\psi) - g(M_0,\psi_0) = 0 = \left.\frac{\partial g}{\partial M}\right|_{M_0,\psi_0}\Delta M + \frac{1}{2}\left.\frac{\partial^2 g}{\partial\psi^2}\right|_{M0,\psi_0}\Delta\psi^2 + \cdots \tag{20}$$

where $\partial g/\partial\psi$ at (M_0,ψ_0) has been set to 0. It is then apparent that the leading-order behavior of the denominator of I_2 is as $\sqrt{(M - M_0)}$. This is exactly the result of Amiet and is an integrable singularity. Also, as Amiet shows, the special case of $\partial g/\partial M = 0$ results in an increase in the order of the singularity to $M - M_0$. This seems immediately obvious from Eq. (20); however, since $\partial^2 g/\partial\psi^2$ also goes to 0 at (M_0,ψ_0) when $\partial f/\partial M = 0$, higher-order terms in the expansion must be used to find the relationship between ΔM and $\Delta\psi$. More simply, from Eq. (19) the leading-order behavior goes like ΔM when C_1 becomes 0. Incidently, C_2 remains nonzero for the conditions of the strong singularity.

As alluded to previously, Amiet found this logarithmic singularity in his calculations, as ha- Chapman[11] and Tam[12] for sharp leading-edge surfaces. Tam also found that, for a blunt leading edge, the strength of the singularity is increased to an inverse square root. This singular behavior comes about because of the infinity in h' itself rather than the characteristics of the supersonic acoustic planform and is not addressed here.

In analyzing the quadrupole singularity, I_3 becomes important. At the strong singularity, the numerator, which includes the factor $\partial^2 g/\partial\psi^2$, approaches 0 at the same rate as $\partial g/\partial\psi$, leading to a singularity that behaves like an integrated double pole, since the curve approaches $-\infty$ from below and ∞ from above with infinite slope in between.

At other than the strong singularity, that is, when $\partial g/\partial\psi = 0$, but $\partial g/\partial M$ does not equa! zero, the integral of interest behaves like $\int(1/x)(1/|x^{1/2}|)\,\mathrm{d}x$ where the integration must pass through 0. Though the integrand has a $-3/2$ power singularity in it, and is expected to exhibit singular behavior at all observer times for which there is some $M_r = 1$, taking the derivatives outside the integral sign effectively reduces the solution to the "finite part" of the formally improper integral. This does not occur at singularities that behave like $\int 1/|x|\,\mathrm{d}x$,

such as those at the strong singularity in the monopole integral, since the absolute value in the denominator precludes solution using the principal value idea (see, for example, Ref. 13). Therefore, integrals containing singular points of order $1/|x|$ are truly singular in the mathematical sense, and the results do, in fact, show this behavior at the corresponding observer times.

Conclusions

The computed results for monopole and quadrupole waveforms disprove the opinion that numerically differentiating the source integrals in the acoustic analogy equation causes significant errors in determining the waveform shapes and magnitudes. In the monopole case the simple two-point differencing scheme has produced smooth curves that exactly match those computed by moving the derivative inside the integral. Though a new integration grid must be computed for every time step in order to accurately find the value of the integral at that time, this must be done whether or not the integral or the derivative is computed first and does not add any extra steps to the calculation. The foregoing development and results suggest that the current method is superior to making the derivative part of the integrand, since, in the current method, no singular integrations are required.

Whether the source distribution is monopole or quadrupole in nature, true mathematical singularities appear in the waveforms. These occur at observer times corresponding to specific source conditions: A source discontinuity traveling at a rotational Mach number of 1 will emit a singularity-producing pulse when its Mach number in the direction of the observer is also 1. The singular points arise because of discontinuities in the source distribution in the direction of motion. The idealized quadrupole produces a stronger singularity than the monopole because the monopole has only a discontinuity in the slope of the source-defining function, whereas the quadrupole has a discontinuity in the function itself. The appearance of these mathematical infinities may help to explain the universal overprediction of the radiated acoustic pressure using acoustic analogy methods for rotors once shock waves form on the rotor blades and the quadrupole terms become important.

Perhaps the most important conclusion of this work is in the evidence that the linear propagation assumption cannot hope to provide realistic, nonsingular waveforms. The work supports the conclusion that the quadrupole term (and "quadrupole" has indeed been used loosely in the foregoing discussions) is important, not solely as an aerodynamic source, but as a means for providing nonlinear propagation and convection with the flow. As such, the simplification of the term, as proposed in the cited reference, cannot predict what may, in fact, be the most important effect of the Lighthill stress tensor.

References

[1]Ffowcs Williams, J. E., and Hawkings, D. L., "Sound Generation by Turbulence and Surfaces in Arbitrary Motion," *Philosophical Transactions of the Royal Society of London, Series A*, Vol. 264, May 1969, pp. 321–342.

[2]Farassat, F., "Theory of Noise Generation From Moving Bodies with an Application to Helicopter Rotors," NASA TR-R-451, Dec. 1975.

[3]Farassat, F., "Theoretical Analysis of Linearized Acoustics and Aerodynamics of Advanced Supersonic Propellers," AGARD CP-366, 1985, pp. 10-1–10-15.

[4]Farassat, F., "Prediction of Advanced Propeller Noise in the Time Domain," *AIAA Journal*, Vol. 24, April 1986, pp. 578–584.

[5]Farassat, F., and Brentner, K. S., "The Uses and Abuses of the Acoustic Analogy in Rotor Noise Prediction," *Journal of the American Helicopter Society*, Vol. 33, Jan. 1988, pp. 29–36.

[6]Farassat, F., "Quadrupole Source in Prediction of the Noise of Rotating Blades—A New Source Description," AIAA Paper 87-5225, Oct. 1987.

[7]Amiet, R. K., "Thickness Noise of a Propeller and its Relation to Blade Sweep," *Journal of Fluid Mechanics*, Vol. 192, July 1988, pp. 535–560.

[8]Wells, V. L., "Analysis of the Acoustic Planform Method for Rotor Noise Prediction," *AIAA Journal*, Vol. 26, May 1988, pp. 522–523.

[9]Schmitz, F. H., and Yu, Y. H., "Helicopter Impulsive Noise: Theoretical and Experimental Status," NASA TM-84390, Nov. 1983.

[10]Gel'fand, I. M., and Shilov, G. E., *Generalized Functions: Properties and Operations*, Vol. 1, Academic, New York, 1964.

[11]Chapman, C. J., "Whitham's *F*-function in Supersonic Propeller Acoustics," AIAA Paper 89-1107, April 1989.

[12]Tam, C. K. W., "On Linear Acoustic Solutions of High Speed Helicopter Impulsive Noise Problems," *Journal of Sound and Vibration*, Vol. 89, July 1983, pp. 119–134.

[13]Edwards, J., *A Treatise on the Integral Calculus*, Chelsea, New York, 1954.